Thermal Camera for Autonomous Mobile Platforms

Grzegorz Bieszczad, Michał Krupiński, Henryk Madura, and Tomasz Sosnowski

Abstract. Unmanned Aerial Vehicles (UAVs) have found many applications, both civilian and military. They can be used by armed forces, police, border guard, customs office, search and rescue units but also in scientific research, power and civil engineering and environmental monitoring. However, regardless of actual application, there is always a requirement for an observation system capable of providing visual data in low light, harsh weather conditions and during nighttime. In the paper the construction of high resolution thermal camera is presented, fitted with microbolometer 640x480 focal plane array operating in 8÷12 μm spectral range. This lightweight and energy efficient device can be mounted onboard an UAV for observation, target detection and recognition in difficult weather and low light conditions and in low visibility situations caused by dust, smoke or fog. The described camera provides full day/night observation capability.

1 Introduction

There are many situations in which UAVs are used as an element of surveillance system, delivering valuable data on actual situation and objects over monitored area. To fulfill such a task, UAVs are usually equipped with various types of sensors and cameras to ensure detection, recognition and identification of phenomena and objects regardless of weather conditions and time of day. A thermal camera with high spatial resolution is a perfect example of an imaging sensor that can significantly enhance the detection, recognition and identification capability of an observation system, which in turn can be simplified and even automated [1, 2, 5, 10, 14]. Simultaneous analysis of image data in two information channels (visual and infrared) gives both the possibility of night operation and increases the

Grzegorz Bieszczad · Michał Krupiński · Henryk Madura · Tomasz Sosnowski
Military University of Technology, Institute of Optoelectronics,
Warsaw, Poland
e-mail:{tsosnowski,hmadura,gbieszczad,mkrupinski}@wat.edu.pl

A. Nawrat and Z. Kuś (Eds.): *Vision Based Systems for UAV Applications*, SCI 481, pp. 95–114.
DOI: 10.1007/978-3-319-00369-6_6

effectiveness of implemented algorithms for object identification [2, 10, 11]. The application of a thermal camera gives also the possibility to assess the current status and the previous actions of objects by analyzing their thermal signatures (e.g. barrel temperature or engine temperature) [1, 2, 14]. It is also possible to detect concealed, camouflaged objects. It is then possible to mount a high resolution thermal camera with a focal plane array (640x480 pixels, 17 μm pixel pitch, spectral range 8÷12 μm) onboard an UAV. Devices designed for UAVs should be lightweight, small and energy-efficient, so an uncooled microbolometer focal plane array was chosen for the onboard thermal camera. Due to constant progress in microbolometer detector technology its current generation provide high sensitivity, small pixel size and lowered power consumption. Most significant advantage of microbolometer detectors is their ability to work at ambient temperature.

2 General Construction of High Resolution Thermal Camera

High resolution, observation thermal camera is meant for area surveillance and target detection in any time of day, regardless of light conditions and weather (including light fog or smoke) [2]. Cross section and real photo of the designed high resolution thermal camera is presented in Fig. 1.

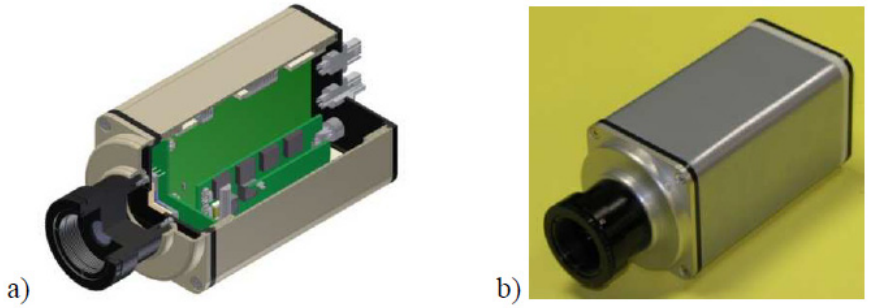

Fig. 1. CAD project (a) and real photo (b) of high resolution thermal camera

The following elements can be distinguished in the construction of a thermal camera: lens (specially designed for infrared spectral range), focal plane array (FPA), digital image processing and control module, power supply and video display module [12, 13]. General block diagram of a thermal camera is presented in Fig. 2.

Power supply must feed the various camera component and meet very strict noise requirements. During the design of power supply for the camera with microbolometer FPA it was necessary to provide several different voltages supplying different camera components. All those voltages are obtained from single external supplying voltage by using switched mode power supplies instead of linear regulated ones. It increased the efficiency and resulted in lower heat dissipation inside

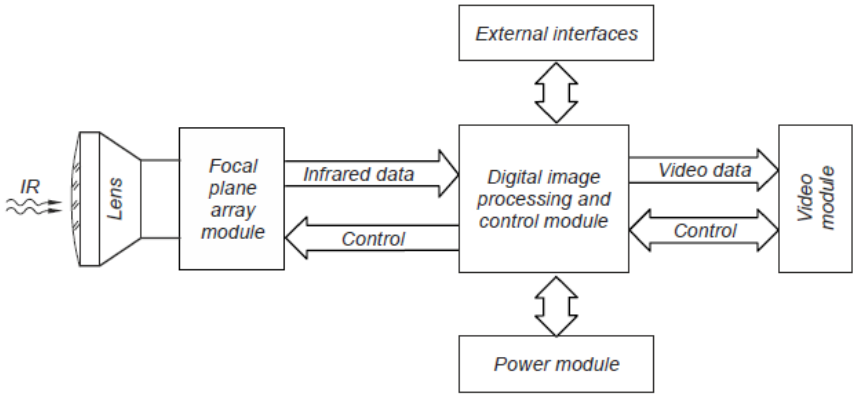

Fig. 2. General block diagram of a thermal camera with all main functional blocks

the camera case. Low power operation and the flexible range of external supplying voltages are also important features of the presented camera. It was assumed, during the design of camera electronic modules, that the camera will accept supplying voltages in the 6V – 12V range. The device can be supplied from typical regular or rechargeable batteries thus allowing the camera to be applied even in mobile systems with autonomous power sources of limited capacity.

2.1 Lens Module

Objective lens for far infrared spectral range is one of the most technologically sophisticated camera components. Its complexity is caused by the requirements for wide field of view, small overall dimensions, wide range of operating temperatures, anti-reflex coatings resistant to environmental conditions and the resolution matching 17 µm pixel pitch of a FPA. Those requirements imposed the application of modern design approach and materials. The lens features aspherical germanium optical elements which reduced the total number of optical elements in the lens design. And due to wide temperature range the passive athermalization of the lens was necessary.

Each optical system is prone to misalignment due to temperature changes. Ambient temperature variations significantly affect the imaging quality of far infrared lens, because of material properties, such as coefficient of thermal expansion and thermal coefficient of refraction. As a result dimensions of mechanical and optical elements as well as optical properties of germanium change with temperature. Usually both those undesired effects do not compensate themselves but they are additive. As a result the focal length is shortened as the temperature rises. Furthermore the FPA itself, due to thermal expansion of the case and mount, is moved away from the reference focal plane.

In order to create the lens operating within 1/4 wave Raleigh criteria in the whole -40C° to +60C° temperature range the particular elements were designed in

such a way to provide compensation of both aforementioned undesired effects. The applied passive athermalization was achieved through certain design solutions and application of materials with appropriate thermal expansion properties, which made it possible to obtain compensation movement of desired magnitude. As a result the optical system was created with the following parameters:

- Focal length 12mm,
- Field of view (for 640 x 480 FPA, 17 um pixel pitch): HFOV~49 VFOW~38
- F-number 1.25,
- weight 29.5g.

It was confirmed during research that the use of a single aspherical lens provides good imaging quality, light weight and simplified mechanical mount of the resulting obje tive lens. Thus, in spite of complex dual-housing structure the compact unit was obtained and applied athermalization is sufficiently effective in the whole range of operating temperatures. Limiting the number of optical surfaces is also beneficial in terms of transmission losses, which is particularly important in infrared optical sys-tems made of germanium, a material with high refractive index. The losses can be minimized by lens coatings, but the reduction of the number of optical elements is also important. The resulting objective lens, in spite of a fairy large field of view, provides quite uniform illumination of a focal plane array.

2.2 Focal Plane Array Module

Focal plane array module is the next one of the technologically advanced camera blocks. It is composed of a microbolometer focal plane array and a PCB board with read-out, control and power supply circuits.

In the presented high resolution thermal camera the FPA made of amorphous silicon was applied. It is an uncooled infrared detector and its spectral range is defined by an optical filter, mounted as an outer cover of a detector case.

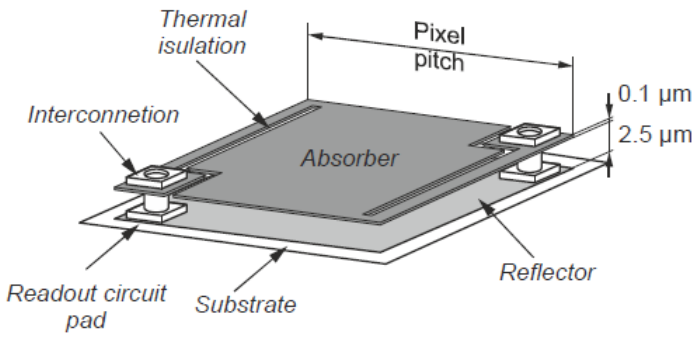

Fig. 3. Single pixel of a microbolometer focal plane array

The applied infrared FPA has 640 by 480 single IR detectors (bolometers) . An active bolometer is made of a silicone membrane covered by an IR absorber. A single detector is a micro electro-mechanical structure. In such structure the detecting element is physically (and thermally) insulated from the rest of the components, including FPA housing. The schematic construction of a single detector in microbolometer array is shown in Fig. 3.

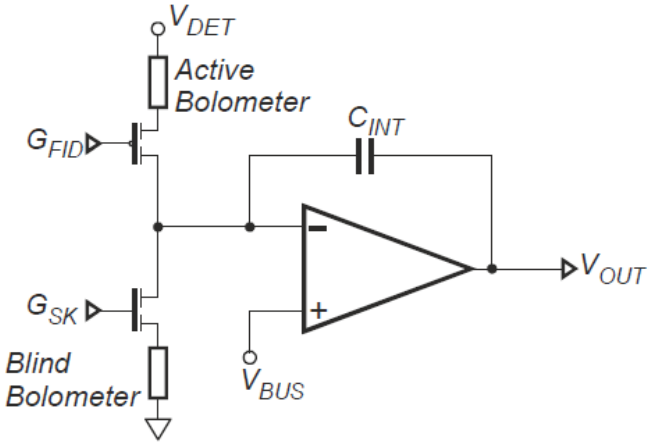

Fig. 4. Simplified diagram of a single pixel read-out circuit

Each individual bolometer is connected to a read-out circuit, which converts the resistance changes into proportional electric signal (voltage). The resistance variations are caused by temperature change of an active bolometer, introduced by total FPA temperature and incident infrared radiation. The conversion of bolometer resistance into voltage signal is performed in a circuit depicted in Fig. 4.

Current-to-voltage converter is applied to obtain electric signal from individual bolometers. The charging current of integrator capacitance C_{INT} is defined by the voltages V_{DET} and V_{BUS} and the resistances of a bolometer and MOSFET transistor. Integration time is set depending on actual frame rate. The portion of total bolometer resistance resulting from bolometer own temperature is also included in the conversion process. To determine its value the "blind" bolometer is applied, covered from incident radiation. Voltages G_{SK}, G_{FID}, V_{DET} and V_{BUS} that directly influence the output signal are shown in Fig. 4. The level of those voltages as well as precision and resolution of their setting determine the dynamic range and the quality of output image. As a result those voltages (values and noise levels) are strictly defined by a FPA manufacturer. Noise parameters of analogue supplying voltages are particularly important and they are defined by manufacturer over specified frequency bands. Allowed values are presented a table 1.

Table 1. Noise requirements for FPS supplying voltages

Voltage	Noise level	Measurement band
V_{BUS}	100 μV	1 Hz ÷ 10 MHz
G_{FID}, V_{DET}, G_{SK}	2 μV	1 Hz ÷ 10 MHz
	5 μV	1 Hz ÷ 10 kHz
	100 μV	1 Hz ÷ 10 MHz

Generally speaking, focal plane array module must provide analogue and digital supplying voltages for an array, analogue control signals for a FPA and buffering of digital control signals. This module should also include analog output stage.

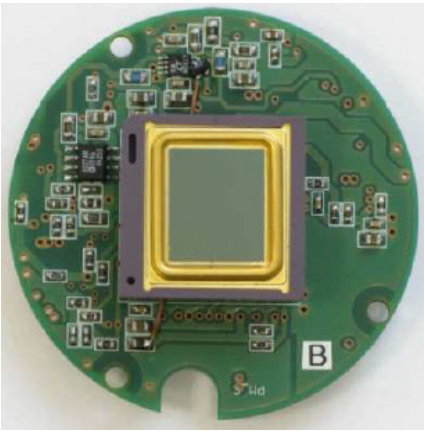

Fig. 5. Photo of a PCB board with FPA array (17 $\boldsymbol{\mu m}$ pixel pitch)

In the presented camera a state-of-the-art array awas applied, with 640x480 pixels and 17 μm pixel pitch. Due to small pixel size (and consequently smaller linear dimesions of an array) the size of objective lens could be reduced, which also contributed to lower weight of the whole camera. In Fig. 5 the printed circuit board is shown with mounted focal plane array.

3 Digital Image Processing and Control Module

In high resolution thermal cameras the fast image processing system has to be applied, which combines significant processing speed with a low power consumption. Additionally modern system has to be flexible, ready to perform different tasks wit out significant hardware modifications. Digital processing in high resolution cameras involves considerable amount of data, which must be processed within defined time window [8, 12, 13]. Data should be processed on the fly (in real time) without introducing excess latencies. For the continuity of data processing the system latencies should be constant, i.e. they cannot cumulate over time. This requires parallelization of image data processing.

Main tasks performed by digital image processing and control module are: controlling the array in order to read-out the values of detector signals, correction of detector non-uniformity (NUC), bad pixel mapping and preparing the data for video display module.

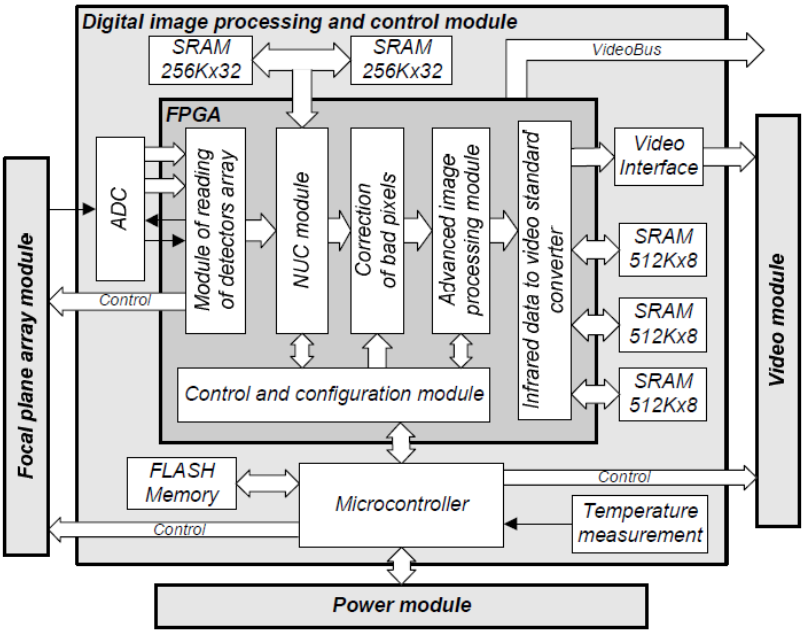

Fig. 6. Functional block diagram of FPGA-based digital image processing and control module

The module was constructed around two main integrated circuits: Field Programmable Gate Array (FPGA) and a microcontroller. Programmable FPGA integrated circuit realizes image processing, which demands considerable processing power. The main tasks of FPGA device are: generating timing signals for infrared array, performing non-uniformity correction, replacement of so-called bad pixels and generation of signals for video display module. Microcontroller is responsible for controlling of all modules in camera and participates in other tasks that do not demand significant processing power. The block diagram of control and image processing module with FPGA device is shown on a Fig. 6, and the photo of the real camera module is presented in Fig. 7.

The main tasks of microcontroller is supervising the image processing chain on every step and communicating with interfaces connected to camera. In particular he microcontroller is responsible for configuring and adjusting biasing voltages for detector array, measuring the FPA and ambient temperatures, controlling the shutter and the process of auto calibration, configuring of video display, modifying and calculating coefficients needed for non-uniformity correction algorithm.

Fig. 7. Printed circuit board of FPGA-based digital image processing and control module

As the microprocessor for the control and image processing module the LPC2292 from NXP was chosen, which is a member of 32-bit ARM7 family. This microcontroller is based on 32-bit CPUs of ARM7TDMI-S type, with 256 kB of internal flash memory. It has 128 bit internal memory interface and unique architecture capable to execute 32-bit program code with high efficiency. It also has low power consumption and rich set of peripherals like 10-bit analog-to-digital converter, 32 timers and communication modules compatible with standards like SPI, I2C, CAN and UART. What is more, a LPC2292 microcontroller has a sufficient number of general purpose input-output (GPIO) ports and external memory interface. The connection between microprocessor and a FPGA circuit by a special communication bus was supported by this last interface.

4 Image Processing Modules Implemented in FPGA

Because of rather high computation power demands and parallelization of image processing, FPGA device EP2C35F672 from ALTERA was applied in control and image processing module . This FPGA integrated circuit provides adequate speed and relatively low power consumption. Applied FPGA device has large number of IO ports, 33 216 logic elements (LEs), 483 840 bits of internal RAM memory, four PLL circuits that allows to generate a series of precision timing signals and 35 hardware multipliers for DSP operations. Hardware multipliers are necessary for building fast and sophisticated digital processing modules consuming low amount of logic resources and with low power demands. In FPGA device the following modules were implemented for the needs of real-time image processing: detector array readout module [12, 13], NUC module [4], bad pixel replacement module, image processing module and image display module.

4.1 VideoBus

In FPGA circuit a special bus was designed to interface image processing modules with each other. All modules implemented in FPGA structure are exchanging image data via VideoBus link, what is schematically illustrated in Fig. 8.

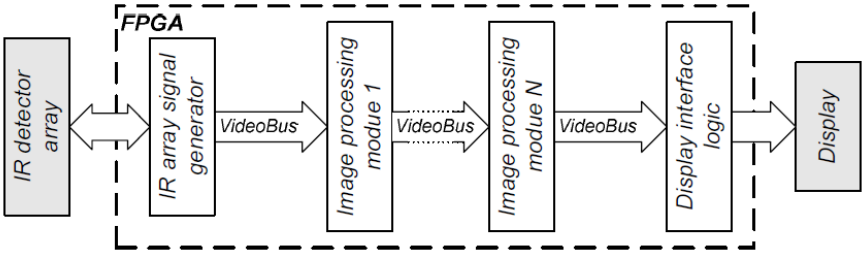

Fig. 8. Block diagram of data processing chain implemented in FPGA

Thanks to uniform VideoBus interface there is a possibility to change the order of executed image processing operations without any need of modifying the modules. The modules are designed in such a way that they can be made transparent to incoming data, passing data through without modification. This feature allows to dynamically control the image data processing.

VideoBus link is composed of 14-bit video data bus (VDATA), vertical synchronization signal (VSYNC), horizontal synchronization signal (HSYNC) and strobe signal (STB). Vertical synchronization signal (VSYNC) is high during transfer of the frame signal. Horizontal synchronization signal (HSYNC) is high during transfer of data related with single line in the frame. The change of strobe signal from low to high state (leading edge) indicates valid data on the Video data (VDATA) bus that is ready to be received. Data on VDATA bus are maintained during the high state of STB signal. VSYNC and HSYNC signals assume high state before the occurrence of first leading edge of STB signal. Timing diagram of signals over VideoBus link are presented in Fig. 9.

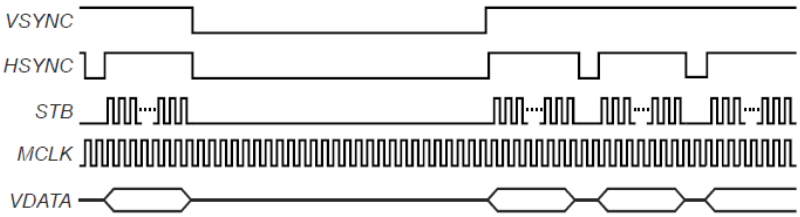

Fig. 9. Timing diagram of signals in VideoBus

4.2 Detector Array Readout Module

The main tasks of detector array readout module is generation of signals driving internal circuitry of detector array to enable reading the signals from all consecutive detectors (pixels). Designed circuit generates the appropriate control signals in a proper sequence, which causes the array output signal to appear at analog or digital output terminal. This signal is a response of the detector and is proportional to the incident infrared radiation.

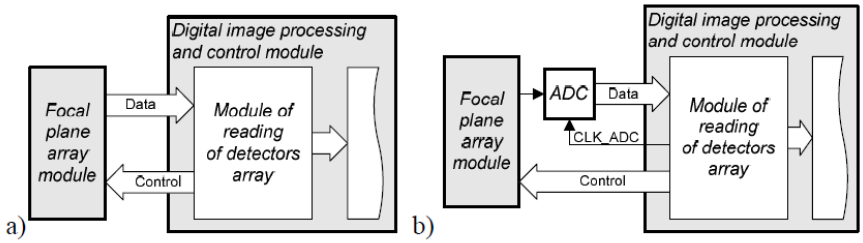

Fig. 10. Read-out circuit for an FPA array with digial (a) and analog (b) output

There are two types of detector array readout interfaces. One is a digital interface, when the array has internal analog-to-digital converter [13]. The block diagram illustrating the connection to such device is presented in Fig. 10a. The main advantage of that solution is that there is no additional ADC element present in the device. This can simplify the design, but the use of an internal ADC can sometimes have a negative impact on NETD parameter of the camera.

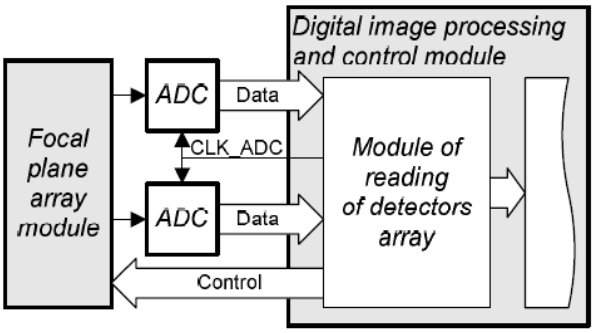

Fig. 11. Read-out circuit for an FPA array with dual analog output

The second interface type is the analog one. In this case an external analog-to-digital converter is necessary to connect analog array output to digital processing system. The block diagram of this solution is shown in Fig. 10b. Read-out module generates control signals not only for an array, but also for ADC converter. Additionally the input range of a converter must be adjusted to the dynamic range of array output. This gives the designer full control over the dynamic range of output signal High resolution infrared arrays (640x480 and higher) have commonly more than one analog output (usually two or four), providing simultaneous readout from several detectors. For this type of arrays there is a need to interface to all outputs using several synchronized analog-to-digital converters. An example readout system with two channel analog-to-digital converter is shown in Fig. 11.

In general the readout circuit contains a buffer and ADC converter. On Fig. 10 and Fig. 11 both elements were schematically illustrated as one functional block – an ADC converter. In fact the analog output of dete tor array has strictly defined

parameters like output impedance and possible output current. That is why it cannot be loaded with resistance lower than nominal (for example 100 kΩ). The majority of fast analog-to-digital converters have low input I pedance, so separate buffer is necessary. Additionally the buffer can be used to adjust the dynamic ranges of both devices – detector array and ADC. The most important parameters of ADC are resolution and speed. Sampling frequency of a converter depends on array design (readout speed and the number of outputs) and on frame rate. The required resolution of ADC is a result of signal to noise ratio (*SNR*) at the output of detector array If the amplitude of the noise in the array is U_N, the amplitude of the signal is U_S, then the *SNR* is given by:

$$SNR = \frac{U_S}{U_N} \tag{1}$$

and the minimal resolution of ADC converter can be then calculated according to the formula:

$$N \geq log_2(SNR), \tag{2}$$

where N is a minimal bit count of ADC converter word.

Digital signals driving detector array, has to be generated for every type of the detector. The task is complex, because different types of detector arrays have different interfaces and demands different signals and timings, even in case of the same manufacturer. A block diagram of UL 04 27 2 detector readout module realized as a FPGA functional block is shown in Fig 12.

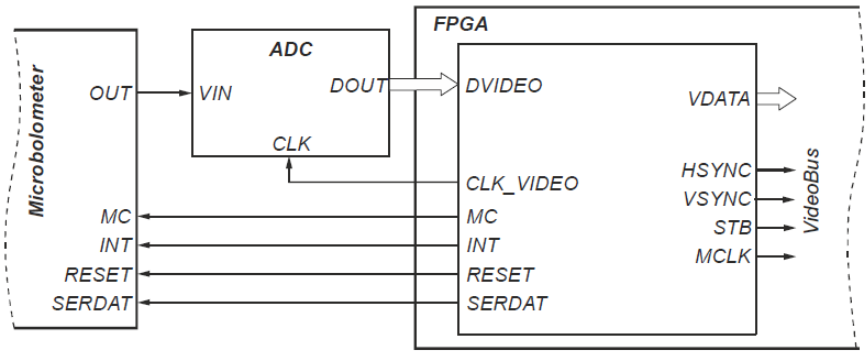

Fig. 12. Block diagram of read-out control module for ULIS' UL 04 27 2 microbolometer FPA

The digital signals for controlling the microbolometer array can be divided into two groups. One is to provide proper timing during readout from detectors whereas the second is used for array configuration. First group includes RESET, INT, MC and CLK_VIDEO. Execution of the module results in reading all the pixel values which are then sent for further processing via image data bus [8, 12, 13]. Example signal diagrams for UL 04 27 2 array are shown on Fig. 13.

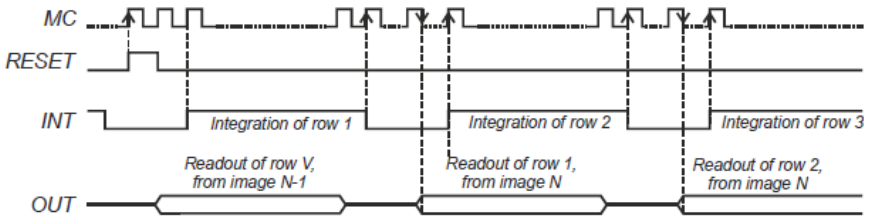

Fig. 13. Timing diagram of control signals for ULIS' UL 04 27 2 microbolometer FPA

A special control circuit was designed to read the signals from the particular detectors in an array. Its purpose is to obtain for of each detector signal proportional to incident IR radiation its digital representation. Data is further sent to other camera blocks by VideoBus link. All analog detector signals (OUT) need to be converted into digital form (DVIDEO). Conversion was performed by ADC converter, which requires clock signal (CLK_VIDEO).

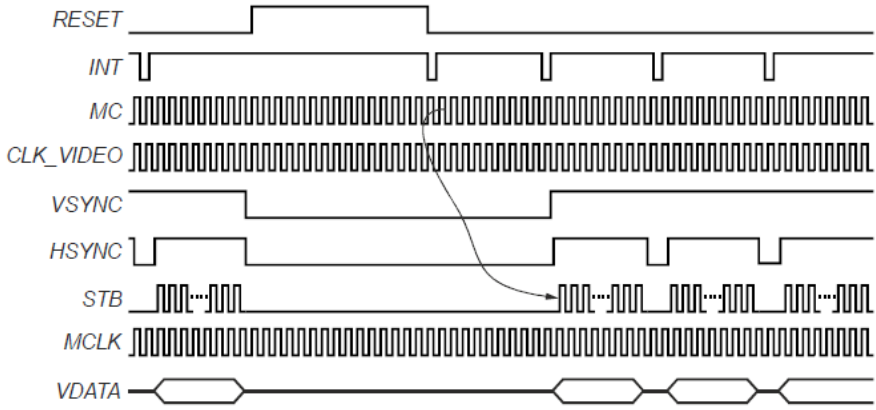

Fig. 14. Timing diagrm of control signals for ULIS' UL 04 27 2 microbolometer FPA

According to array catalogue data all control signal can be generated using single clock signal with MC period. To do this a module was realized with 5-state machine and two synchronous counters. First counter is used to determine the states of RESET signal and for counting clock cycles during the readout of an entire frame. Second counter is used to determine the states of INT and MC signals and performs cycle count during single row readout. On the basis of RESET, INT and MC signals the following VideoBus signals are simultaneously generated: VSYNC, HSYNC, STD, MCLK, VDATA. During the operation of UL 04 27 2 microbolometer array the signals on the output of array are delayed by the time of one row from the integration trigger signal. This is because at the beginning of each frame readout the signals from first row detectors are integrated. Then, during the readout of first row detectors the signals from second row detectors are integrated and the pattern is repeated for the consecutive rows. As a result the total

number of signals for row readout is larger by one than the total number of rows in the array. Example signals generated for microbolometer array are shown on Fig. 14.

The applied ADC converter AD9251 from ANALOG DEVICES has its own latency needed to process incoming analog signal that equals to 9 clock cycles. This means that the result of analog-to-digital conversion is available after tenth measurement is triggered.

4.3 Bad Pixel Replacement Module

Practically in all detector arrays here are some detectors that are not working properly, thus the signal from detected bad pixel has to be eliminated and replaced. During the calibration process the defective pixels are identified when they return incorrect signal value. On this basis the bad pixel map is stored in memory, where every bit corresponds to one detector in an array. If the detector is recognized as bad (meaning its output needs to be corrected) then the corresponding memory value is '1'. In case of good detector (no correction required) the value is '0'. The memory value is used to determinate if the signal from the detector will be displayed. For faulty detector the output value of previous good pixel is substituted instead. The simplified architecture of module realizing this algorithm is shown on Fig. 15.

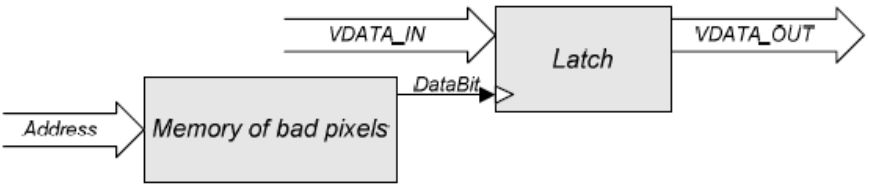

Fig. 15. Operation of bad pixel replacement module

4.4 Video Module

One of the problems encountered in digital image processing is the case when the read-out rate of an array differs from displaying frame rate. And for thermal cameras the displaying frame rate is usually higher. Thus the special module has to be applied, which simplified operation is schematically presented in Fig. 16.

Video module uses two external memories SRAM 1 and SRAM 2. Data from single frame is written to one of the memories (for example SRAM 1). At the same time data to be displayed is being read from second memory (SRAM 2). When whole data from single frame is entirely stored in the first memory, special "Memory select" signal is triggered and the roles of SRAM 1 and SRAM 2 memories are reversed. Now the next frame data is being written to SRAM 2 memory and SRAM 1 data is being read and displayed.

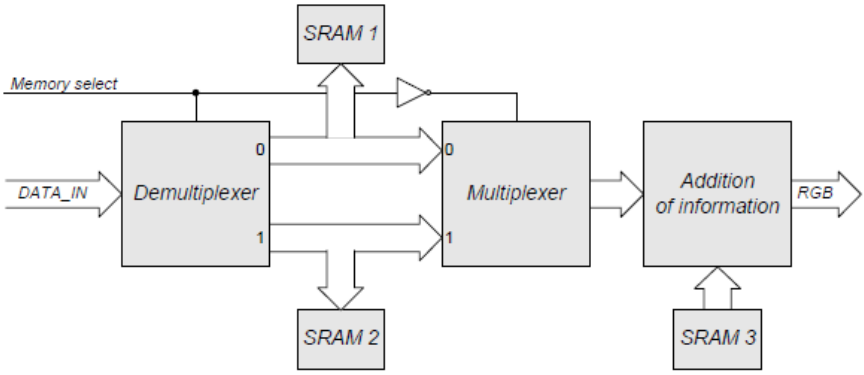

Fig. 16. Operation of module for video displaying and adding additional information to output video data stream

Another function performed by this module is adding additional information to independent video stream. This function is used to implement user interface and to show vital information like e.g. battery level. The video module includes also VGA controller which provides signals for an external display.

4.5 Non-uniformity Correction Module

Infrared detector array always exhibits characteristic non-uniformity of detector responses to uniform incident radiation power [3, 4, 6, 7, 9]. Microbolometer FPA, features unwanted detector gain and offset differences between particular pixel detectors. It is caused by imperfection of individual detectors and readout circuit, characteristic to used technological process as well as array temperature. The effect of non-uniformity of detectors in an array is so called Fixed Pattern Noise (FPN) superimposed on the output image, which decreases the spatial NETD of a thermal imaging camera.

Non-uniformity correction (NUC) consists in digital conversion of output signal from an array in order to eliminate FPN in resulting thermal image. To eliminate non-uniformity effects in the camera, various NUC methods are employed. The most common approach is to process the data from detector digitally. Correction data (NUC correction coefficients) are determined during calibration process where dete tors are exposed to uniform infrared radiation references.

The most principal non-uniformity correction method is so called two-point correction (TPC) algorithm. TPC algorithm is realized according to the formula [4, 7]:

$$Y_{ij}^{*} = G_{ij} Y_{ij} + O_{ij} \tag{3}$$

where Y_{ij} is a digital value of detector response from *i-th* row and *j-th* column (i, j), G_{ij} and O_{ij} are respectively a gain and offset correction coefficients, and Y_{ij}^{*} is a corrected value. NUC coefficients for two point correction are calculated during calibration according to formulas [4, 7]:

$$G_{ij} = \frac{Y(T_H) - Y(T_L)}{Y_{ij}(T_H) - Y_{ij}(T_L)}, \tag{4}$$

$$O_{ij} = \frac{Y(T_L)Y_{ij}(T_H) - Y(T_H)Y_{ij}(T_L)}{Y_{ij}(T_H) - Y_{ij}(T_L)}, \tag{5}$$

where $Y_{ij}(T_H)$ and $Y_{ij}(T_L)$ are digital values of detectors response for higher (T_H) and lower (T_L) temperature of uniform reference black body, $Y(T_H)$ and $Y(T_L)$ are mean values of array response for temperatures TH and TL of black body, given by:

$$Y(T) = \frac{1}{MN}\sum_{i=1}^{M}\sum_{j=1}^{N} Y_{ij}(T)\,. \tag{6}$$

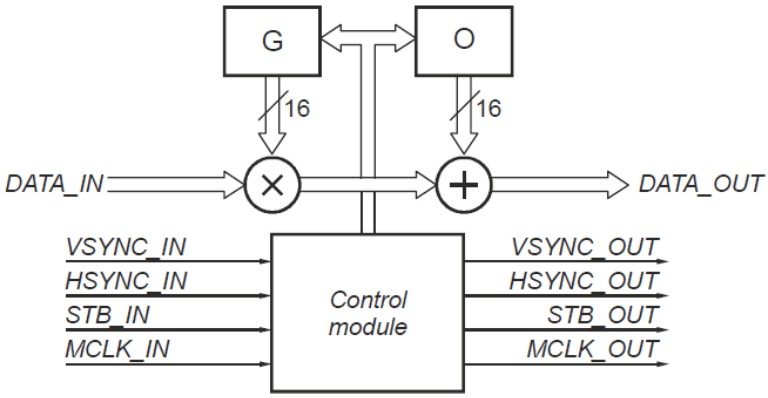

Fig. 17. Block diagram of a hardware NUC correction

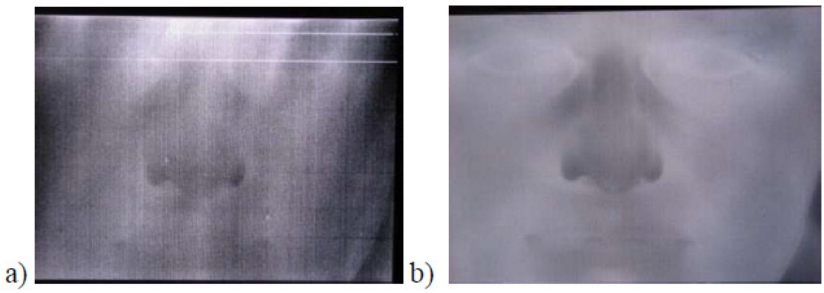

Fig. 18. Sample thermal image before (a) and after (b) NUC correction

On the basis of analysis and simulations the 14-bit resolution of video data (resolution of ADC converter) and 16-bit correction coefficients were adopted [3, 4]. From equation (3) came off that the digital module realizing TPC algorithm

has to make one multiplication and one addition operation. To increase the precision of NUC calculations (which are made on fixed-point digits) the coefficients must be resized accordingly. Block diagram of hardware realization of TPC algorithm for thermal camera is presented on Fig. 17.

In this hardware realization the correction is realized “on the fly”. Time of calculation is shorter than the time between reading succeeding detectors. The module is designed to have inputs and outputs compatible with internal VideoBus link. Non-uniformity correction module was described in VHDL language as a parameterized entity. D signer can change (when needed) the parameters of the module like size of actual infrared detector array, length of video data word and length of coefficient data word. Because of that feature this module can be used for any array size. Fig. 18 shows two thermal images: one taken before and one after NUC correction performed by the described module.

5 Calibration, Measurement and Determination of Thermal Camera Parameters

Procedure used to determine the correction coefficients according to TPC algorithm is performed on a test stand [9] with two blackbodies at temperatures TL and TH, respe tively. The stand with mounted camera is kept at constant ambient temperature (e.g. in climate chamber). After switching on the camera, prior to measurements it is ne essary to wait until the array and camera housing temperatures stabilize. Then the calibration procedure may begin. The test stand used for the determination of NUC coefficients is shown in Fig. 19. Averaged array response values for TL and TH temperatures, used for NUC coefficient calculations, are called calibration points. Basic calibration points are the array averaged responses for the temperatures TL = 20°C and TH = 40°C. Calculated correction coefficients Gij i Oij are stored in camera’s internal memory. In each detector array a faulty pixels (detectors) can be found, due to manufacturing defects. Those detectors, referred to as “bad pixels” are usually found during calibration. There are several ways to identify bad pixels:

- on the basis of detector gain,
- on the basis of detector offset,
- on the basis of detector noise.

Identification of bad pixels on the basis of detector gain is performed using a threshold value. A pixel is considered bad if its gain coefficient in a NUC table differs from nominal value by more than selected percentage value. For example, if the threshold value is 25% then all the detectors with gain coefficients below 0.75 and above 1.25 are considered bad.

Fig. 19. Test stand for determining NUC correction coefficients and bad pixel identification in microbolometer focal plane array

Fig. 20. Test stands for the determination of parameters of thermal cameras (Accredited Laboratory of Institute of Optoelectronics, MUT)

Similarly the identification of bad pixels on the basis of detector offset is carried out. Pixel is considered bad if its offset correction coefficient in NUC table is smaller or greater than defined percentage value (e.g. 30%).

Using detector noise criteria the pixel is marked as bad if its noise level (RMS) exceeds the defined threshold value. For example, for a given noise level (mean value of 5.0 and standard deviation of 1.0) and a threshold set at 3.5, the pixel is considered bad when its RMS noise value exceeds 8.5.

The measurements of basic parameters of the presented thermal camera were performed at the Institute of Optoelectronics on the specialized test stand for the evaluation of thermal cameras [9]. The test stand consists of a collimator, IR radiation standards with control units, rotating test and filter wheels and a computer with video grabber card and specialized software (Fig. 20).

The following camera characteristics were measured on this test stand:

- modulation transfer function MTF,
- signal transfer SiTF,
- minimum resolvable temperature difference (MRTD) characteristics,
- 3D noise model.

MTF function describes the image distortions introduced by a camera. It is defined an a module from normalized to unity FFT transform of luminance distribution in a point source image, for null spatial frequency.

On the basis of derived MRTD characteristics the detection, recognition and identification ranges were calculated for a standard NATO target, according to STANAG 4347. Spatial noise of an imaging system can be calculated using 3D noise model. Each noise component of a system influences the image quality. The analysis of the contribution of each particular noise source is difficult, or rather impossible, as the influence of different noise sources may result in the same type of image degradation. Thus in order to perform noise analysis the 3D noise model was introduced.

In order to determine 3D noise components several images of uniform background were acquired and on this basis the matrix noise model of camera system was created.

6 Summary

The presented high resolution thermal camera with microbolometer focal plane array made of amorphous silicon operates in 8-12 μm spectral range. The applied FPA array, made by ULIS (France), has a size of 640x480 pixels, which amounts to the total number of 307 200 infrared detectors. Thermal resolution is 0.08 degrees Celsius and spatial resolution reaches 1.35 mrad. Such parameters allow for the detection of a human being from over 1300 meters' distance. The camera is equipped with atheromalized lens with single FOV of about 50° and F-number of 1.25. The applied passively athermalized lens can operate in a broad temperature range without the need of man al refocusing.

Fig. 21. Sample image produced by the presented high resolution thermal camera

High resolution of the applied focal plane array together with relatively high thermal sensitivity allowed to achieve quite long detection, recognition and identification ranges. The observations of real objects were performed during field tests in various visibility conditions. Sample thermal image of a group of persons and passenger cars is shown in Fig. 21.

The developed camera is a small, lightweight and efficient device with low power consumption. It can be applied in surveillance, reconnaissance and defense systems mounted onboard unmanned aerial vehicles.

References

[1] Kastek, M., Sosnowski, T., Orzanowski, T., Kopczyński, K., Kwaśny, M.: Multispectral gas detection method. WIT Transactions on Ecology and the Environment 123, 227–236 (2009)

[2] Madura, H.: Method of signal processing in passive infrared detectors for security systems. Computational Methods and Experimental Measurements, WIT Transactions on Modelling and Simulation 46, 757–768 (2007)

[3] Bieszczad, G., Orzanowski, T., Sosnowski, T., Kastek, M.: Method of detectors offset correction in thermovision camera with uncooled microbolometric focal plane array. In: Proceedings of SPIE - The International Society for Optical Engineering, vol. 7481, art. no. 748100 (2009)

[4] Orżanowski, T., Madura, H., Kastek, M., Sosnowski, T.: Nonuniformity correction algorithm for microbolometer infrared focal plane array. In: Advanced Infrared Technology and Applications, AITA 9, Leon, November 8-12 (2007)

[5] Bieszczad, G., Sosnowski, T., Madura, H.: Improved sum-of-squared-differences tracking algorithm for thermal vision systems. In: Proceedings of SPIE - The International Society for Optical Engineering, vol. 8193, art. no. 81932R (2011)

[6] Venkateswarlu, R., Er, M.H., Gan, Y.H., Fong, Y.C.: Nonuniformity compensation for IR focal plane array sensors. In: Proc. SPIE, vol. 3061, pp. 915–926 (1997)

[7] Zhou, B., Wang, Y., Ye, Y., Wu, X., Ying, J.: Realize multi-point method for real-time correction of nonuniformity of uncooled IRFPA. In: Proc. SPIE, vol. 5640, pp. 368–375 (2005); Booth, N., Smith, A.S.: Infrared Detectors, pp. 241–248. Goodwin House Publishers, New York (1997)

[8] Bieszczad, G., Sosnowski, T., Madura, H., Kastek, M., Barela, J.: Adaptable infrared image processing module implemented in FPGA. In: Proceedings of SPIE - The International Society for Optical Engineering, vol. 7660, art. no. 76603Z (2010)

[9] Sosnowski, T., Bieszczad, G., Madura, H., Kastek, M., Firmanty, K.: The calibration stand for thermal camera module with cooled infrared focal plane array. In: Proceedings of SPIE - The International Society for Optical Engineering, vol. 7660, art. no. 76603Y (2010)

[10] Madura, H., Kołodziejczyk, M.: Influence of sun radiation on results of non-contact temperature measurements in far infrared range. Opto-electronics Review 13(3), 253–257 (2005)

[11] Krupiński, M., Sosnowski, T., Madura, H., Dabrowski, M.: Infrared and visible image registration algorithm [Algorytm syntezy obrazu termowizyjnego z obrazem z kamery wideo]. Przeglad Elektrotechniczny 88(11 B), 83–86 (2012)

[12] Sosnowski, T., Bieszczad, G., Kastek, M., Madura, H.: Processing of the image from infrared focal plane array using FPGA-based system. In: Proceedings of the 17th International Conference - Mixed Design of Integrated Circuits and Systems, MIXDES 2010, art. no. 5551280, pp. 581–586 (2010)

[13] Sosnowski, T., Bieszczad, G., Kastek, M., Madura, H.: Digital image processing in high resolution infrared camera with use of programmable logic device. In: Proceedings of SPIE - The International Society for Optical Engineering, vol. 7838, art. no. 78380U (2010)

[14] Kastek, M., Dulski, R., Trzaskawka, P., Sosnowski, T., Madura, H.: Concept of infrared sensor module for sniper detection system. In: IRMMW-THz 2010 - 35th International Conference on Infrared, Millimeter, and Terahertz Waves, Conference Guide, art. no. 5612447 (2010)